



# Stochastic Collection Equation: Invariant Evolution of the Cloud Droplet–Size Distribution

Jun-Ichi Yano<sup>1</sup>, Marta Waclawczyk<sup>2</sup>, and Maarten H. P. Ambaum<sup>3</sup>

<sup>1</sup>CNRM, UMR 3589 (CNRS), Météo-France, 31057, Toulouse Cedex, France

<sup>2</sup>Institute of Geophysics, Faculty of Physics, University of Warsaw, Warsaw, Poland

<sup>3</sup>Department of Meteorology, University of Reading, UK

**Correspondence:** Jun-Ichi Yano ([jun-ichi.yano@cnrs.fr](mailto:jun-ichi.yano@cnrs.fr))

**Abstract.** The present paper presents a symmetry analysis of the stochastic collection equation (SCE), which describes the evolution of cloud droplets by their coalescence into larger sizes, and eventually to the size of rain droplets. As the main conclusion, the rain formation is *not* a simple consequence of the growth of the size of the droplets. When the given kernel is invariant under a scale transformation, the size distribution of the cloud droplets simply shift towards the larger sizes with time, asymptotically preserving its shape (*i.e.*, *invariance*), and no separate peak in distribution identified as rain emerges. Findings with the symmetry analysis are supported further by numerical experiments.

## 1 Introduction

The stochastic collection equation (SCE) describes the evolution of cloud droplets by their coalescence into larger sizes, and eventually to the size of rain droplets. This equation is also referred Smoluchowski (1917) equation in honor of the Polish scientist, who derived it originally.

The SCE has already been extensively studied since the pioneering work by Twomey (1964, 1966), Berry (1967), Berry and Reinhardt (1974a, b, c), and its basic behavior has well been established: by running SCE initialized with a distribution with a single peak in cloud–droplet scale, a second peak corresponding larger rain droplets emerges. However, as the present paper is going to point out, such a second peak for rain is not automatically obtained by simply running any SCE. More generally, it appears to us that a basic physical understanding on the behavior of SCE is still to be fully developed, although especially an earlier attempt by Berry (1967), Berry and Reinhardt (1974c, d) must be well credited.

With this general goal in mind, the present paper examines the symmetries as mathematical structures of the SCE system. An interest to this aspect of SCE is emerging today (*e.g.*, Xie 2024): such an abstract approach helps better interpreting the behaviors of the SCE simulated numerically. Although the present study only considers some idealized forms of the kernel, the developed methodology of the analysis can, in principle, be applied to more complex and realistic forms of kernel. The abstract analysis also brings basic physical insights of the growth process of the clouds, associated with the stochastic collection process.



25 The present paper more specifically shows that the rain formation is *not* a simple consequence of the growth of the size of the droplets: the size distribution of the cloud droplets simply shift towards the larger sizes with time, asymptotically preserving its shape, and no distinguished distribution identified as rain never emerges, when the given kernel is *scale invariant*, *i.e.*, the form of kernel does not change by transforming the scale of the droplet size. The rain droplets identified by a distinguished peak in droplet–size distribution emerges only when a distinguished kernel form is assumed for the rain scale. The present paper first demonstrates that, due to the scale invariance of the stochastic collection equation (SCE), the resulting evolution of  
30 the size distribution of the droplets does not change by stretching both in time and size, so long as the collision kernel is also scale invariant (*i.e.*, homogeneous: Fournier and Laurençot 2006).

The scale invariance of SCE can directly be demonstrated by transformation of the variables, with invariance conditions. Some explicit forms of the similarity solutions — the solutions that satisfy the invariances — are further derived by adopting asymptotic expansion methods. Tendency of the SCE system approaches an invariant state of similarity solutions is finally  
35 demonstrated by numerical simulations. As a simple implication from the scale invariance of SCE, a conventional distinction between cloud and rain droplets in microphysics does not arise from a simple difference in their sizes. Rather, the difference arises only by introducing either a scale dependence to the collision kernel or another physical process that is not included in the SCE, such as a loss of rain droplets by fall.

It is fair to say that the existence of the similarity solutions with the SCE is already well known in the meteorology litera-  
40 ture. However, those similarity solutions are often even not mentioned as such, but rather called *self-preserving distributions* (*e.g.*, Friedlander 1961: see also Sec. 11.7.2 of Pruppacher and Klett 1997). Moreover, in the literature, the main purpose of adopting the framework of the similarity solutions, or self–preserving distributions is to derive an exact solution of the SCE, as systematically reviewed in *e.g.*, Secs. 11.7 and 15.3 of Pruppacher and Klett (1997). In contract, the focus of the present paper is on the generality of the similarity solutions as as approximations rather than as exact solutions: those solutions are suggested  
45 to be universal, being derived by symmetry of the system so that physical implications can further be inferred.

There are also already extensive mathematical studies on the symmetry structure of SCE: see *e.g.*, Grigoriev and Meleshoko (1995), Lin *et al.* (2024), and Grigoriev *et al.* (2010) for an overview of more general subjects. Those studies provide a way of deriving exact similarity solutions of SCE in a general manner. However, as will be seen by an example below (*cf.*, Eq. 5.16), those exact solutions tend to be too involved and specific to be useful for general applications. As a result, physical  
50 significance of all those results is not quite obvious either. For this reason, the present paper limits the attention to the simplest transformation rules (*cf.*, Eq. 4.1a, b, c, d) so that the readers can appreciate the advantage of this methodology to infer the physics without overburdened by mathematical complexities.

The present paper emphasizes the relevance of the similarity solutions as asymptotic approximations of the system, as emphasized by Barenblatt (1996), rather than mathematical artifacts. The physical relevance of those similarity solutions are  
55 further demonstrated by directly time integrating the SCE numerically, and showing that the particle–size distribution tends to asymptotically approaches to those similarity solutions with time, in support of the universality suggested by the symmetry analysis.



## 2 Stochastic Collection Equation: Formulation and Nondimensionalization

The stochastic collection equation that describes the evolution of the droplet particles by coalescence in terms of its size distribution,  $n(x, t)$ :

$$\frac{\partial}{\partial t} n(x, t) = \frac{1}{2} \int_0^x n(x-y, t) n(y, t) K(x-y, y) dy - n(x, t) \int_0^{+\infty} n(y, t) K(x, y) dy. \quad (2.1)$$

Here,  $x$  and  $t$  are the droplet mass and the time, respectively;  $K(x, y)$  is the rate that the two droplets with the masses,  $x$  and  $y$ , coalesce into the droplet of the mass,  $x + y$ , which will be referred as *kernel* in the following. Refer to *e.g.*, Sec. 15.3 of Pruppacher and Klett (1997) for the derivation of Eq. (2.1).

We first nondimensionalize the system by setting:

$$x = x_0 \tilde{x}, \quad \tilde{t} = K_0 N_0 t, \quad K(x, y) = K_0 \tilde{K}(\tilde{x}, \tilde{y}), \quad x_0 n(x, t) = N_0 \tilde{n}(\tilde{x}, \tilde{t}), \quad (2.2a, b, c, d)$$

where the variables with the tildes designate the nondimensionalized variables using the factors designated by the subscript, 0. We also define the initial total particle number,  $N_0$ , and the total mass,  $m$ , by

$$N_0 = \int_0^{+\infty} n(x, t=0) dx, \quad m = \int_0^{+\infty} x n(x, t) dx. \quad (2.3a, b)$$

The former is used to nondimensionalize the particle–number density,  $n$ , whereas the latter is conserved with time with the SCE system.

We further normalize the nondimensional variables by the conditions:

$$\int_0^{+\infty} \tilde{n}(\tilde{x}, \tilde{t}=0) d\tilde{x} = 1, \quad \int_0^{+\infty} \tilde{x} \tilde{n}(\tilde{x}, \tilde{t}) d\tilde{x} = 1. \quad (2.4a, b)$$

The first is a direct consequence of the first definition, Eq. (2.3a), above, whereas the second introduces the definition of the particle–mass scale,  $x_0$ , as

$$x_0 = m/N_0. \quad (2.4c)$$

Substitution of Eq. (2.2a, b, c, d) into Eq. (2.1) leads to:

$$\frac{\partial}{\partial \tilde{t}} \tilde{n}(\tilde{x}, \tilde{t}) = \frac{1}{2} \int_0^{\tilde{x}} \tilde{n}(\tilde{x}-\tilde{y}, \tilde{t}) \tilde{n}(\tilde{y}, \tilde{t}) \tilde{K}(\tilde{x}-\tilde{y}, \tilde{y}) d\tilde{y} - \tilde{n}(\tilde{x}, \tilde{t}) \int_0^{+\infty} \tilde{n}(\tilde{y}, \tilde{t}) \tilde{K}(\tilde{x}, \tilde{y}) d\tilde{y}. \quad (2.5)$$

Note that after removing the tilde signs from the nondimensional variables,  $\tilde{x}$ ,  $\tilde{y}$ , etc, Eq. (2.5) becomes identical to the original equation (2.1). This results suggest that the solution of SCE is scale invariant, *i.e.*, the form of this distribution does not change by rescaling the size of the droplets. The conclusion here is due to the fact that Eq. (2.1) does not involve any physical



parameters, when the collection kernel,  $K$ , is treated like one of the dependent variables as in the nondimensionalization here. Thus, the scale invariance suggested here is valid, only if the kernel,  $K$ , is by itself, scale invariant.

85 The result also shows that the nondimensionalization merely serves for a purpose of normalizing the variables by the conditions (2.4a, b). Based on these observations, in the following analysis, the tilde signs are omitted from the above results, yet assuming that variables are already normalized. Note further that the nondimensional total particle number density,  $\tilde{N}$ , is given by

$$\tilde{N} = \int_0^{+\infty} \tilde{n}(\tilde{x}, t) d\tilde{x} = N(t)/N_0 \quad (2.6)$$

The nondimensional total number will be also designated without the tilde sign in the following.

90 Here, pay attention that the tilde signs are introduced again for different purposes in the following. Those should not be confused with the tilde signs temporally introduced for nondimensionalizations in this section.

### 3 Separation of Variables

As a first step of systematically examining the mathematical structure of SCE, a solution with the separation of variables is pursued. This is the simplest manner of obtaining a general solution of a partial differential-integral equation. Thus, we now  
95 set

$$n(x, t) = \tilde{N}(t)\tilde{n}(x) \quad (3.1a)$$

with the normalization condition

$$\int_0^{+\infty} \tilde{n}(x) dx = 1, \quad (3.1b)$$

and  $\tilde{N}(t=0) = 1$ .

100 Substituting Eq. (3.1a) into Eq. (2.1), we obtain

$$\tilde{n} \frac{d\tilde{N}}{dt} = \tilde{N}^2 \left[ \frac{1}{2} \int_0^x K(x-y, y) \tilde{n}(x-y) \tilde{n}(y) dy - \tilde{n}(x) \int_0^{+\infty} K(x, y) \tilde{n}(y) dy \right], \quad (3.2)$$

thus by introducing a separation constant,  $\lambda$ , we obtain separate equations for time and size dependences:

$$\frac{d\tilde{N}}{dt} = -\lambda \tilde{N}^2, \quad (3.3a)$$

$$\tilde{n} = -\frac{1}{\lambda} \left[ \frac{1}{2} \int_0^x K(x-y, y) \tilde{n}(x-y) \tilde{n}(y) dy - \tilde{n}(x) \int_0^{+\infty} K(x, y) \tilde{n}(y) dy \right]. \quad (3.3b)$$



105 Eq. (3.3a) can readily be solved, and:

$$\tilde{N} = \frac{1}{1 + \lambda t}. \quad (3.4)$$

The size distribution is, in principle, also obtained by solving the diagnostic integral equation (3.3b). However, it is immediately found that this system is not self-consistent.

From the constraint (2.4b), we find

$$110 \quad \tilde{N} \int_0^{+\infty} x \tilde{n}(x) dx = \tilde{m}.$$

Here, we have re-introduced the nondimensional total mass by  $\tilde{m}$ , for a clarity of the meaning of the above constraint, though it is unity by definition. From the above, we immediately obtain an expression for the total number,  $\tilde{N}(t)$  by

$$\tilde{N}(t) = \tilde{m} \left[ \int_0^{+\infty} x \tilde{n}(x) dx \right]^{-1}. \quad (3.5)$$

115 However, this conclusion is contradicting, because the left-hand side is time dependent, with its solution given by Eq. (3.4), whereas the right-hand side is constant of time. Thus, a separable solution is not available for the SCE.

This conclusion could also be predicted from a physical intuition: we expect that the peak of the distribution,  $n$ , would move to a larger size with time by following the coalescence growth of the particles. Thus, a “stationary” solution for  $n$ , as defined by separation of variables (3.1a), is not feasible.

#### 4 Symmetry Analysis: Invariant Transforms

120 To further elucidate the scale invariance of the SCE already suggested by the nondimensionalization in Sec. 2 further, we now identify the basic symmetry properties of SCE. More specifically, we focus on the transformations that do not change the form of SCE. A systematic symmetry analysis based on the Lie group is already performed by *e.g.*, Grigoriev and Meleshoko (1995), Lin *et al.* (2024). The purpose here is merely to reproduce basic invariant transformations.

More precisely, we seek the transformation of the variables of the form

$$125 \quad x^* = x/x_0, \quad t^* = t/t_0, \quad K^* = K/K_0, \quad n^* = n/n_0, \quad (4.1a, b, c, d)$$

that keep the governing equation (SCE) invariant. Such a transformation is called the invariant transformation. Here, the transformed variables are designated by \* signs, and constants for transformations by the subscript 0. Note further that the transformation constant,  $K_0$ , for the kernel cannot be chosen arbitrary, but must depends on  $x_0$ , due to its dependency on  $x$  and  $y$ . This constraint will be introduced later.

130 Similarity of the transformation rules (4.1a, b, c, d) to the nondimensionalization procedure, defined by Eq. (2.2a, b, c, d), is worthwhile to note: a close link of the two operations can be shown in a more formal manner (*cf.*, Ch. 1 of Bluman and Kumei



1989). Also recall that the adopted nondimensionalization keeps the governing equation (SCE) invariant. The goal here is to identify a more general transformation rule to maintain such an invariance.

By substituting the transformations (4.1a, b, c, d) into Eq. (2.1), we obtain:

$$135 \quad \frac{n_0}{t_0} \frac{\partial}{\partial t^*} n^*(x^*, t^*) = n_0^2 K_0 x_0 \left[ \frac{1}{2} \int_0^{x^*} n^*(x^* - y^*, t^*) n^*(y^*, t^*) K^*(x^* - y^*, y^*) dy^* \right. \\ \left. - n^*(x^*, t^*) \int_0^{+\infty} n^*(y^*, t^*) K^*(x^*, y^*) dy^* \right]. \quad (4.2)$$

By further posing the condition that those transformation constants do not appear in the final result, so that the transformed equation takes the same form as the original, we identify the condition for the invariant transformation:

$$n_0 K_0 x_0 t_0 = 1. \quad (4.3a)$$

140 A special case to consider is when only the transformation in time (4.1b) and the resulting transformation of the number density (4.1d) by setting  $K_0 x_0 = 1$ . As a result, the condition (4.3a) reduces to:

$$n_0 t_0 = 1. \quad (4.3b)$$

This constraint means that when the time is stretched by a factor,  $c$ , the number density must be reduced as a whole by the factor,  $1/c$ , *i.e.*,

$$145 \quad t^* = ct, \quad n^* = n/c. \quad (4.3c)$$

This invariant transformation is originally explicitly pointed out by Strivastava (1988), although earlier papers implicitly invoke this rule.

Another constraint for the invariant transformation is obtained by further introducing the transformation of the total mass by

$$150 \quad m^* = m/m_0. \quad (4.4a)$$

From the mass conservation (2.3b), we obtain the constraint:

$$x_0^2 n_0 = m_0. \quad (4.4b)$$

This result summarizes Eqs. (2)–(4) of Xie (2024).

Especially, when we seek an invariance transform of the time from  $t = t_1$  to  $t = t_2$  that constitutes an actual evolution of the system,  $m_0$  must be kept constant (invariant by itself). In this case, without loss of generality, we set  $m_0 = 1$ , and

$$x_0^2 n_0 = 1. \quad (4.4c)$$



In the following, we focus on this case in seeking invariant solutions that can describe an actual evolution of the distribution. Eq. (4.4c) can be re-interpreted as a definition of  $n_0$  in terms of  $x_0$ :

$$n_0 = 1/x_0^2. \quad (4.4d)$$

160 By substituting (4.4d) into (4.3a), we find

$$K_0 t_0 / x_0 = 1. \quad (4.5a)$$

We now assume that the form of kernel is also scale invariant, which satisfies a homogeneous form (*cf.*, Fournier and Laurençot 2006):

$$K_0 = x_0^\gamma \quad (4.5b)$$

165 with the transformation constant,  $K_0$ , of the kernel, where  $\gamma$  is a constant to be specified based on a given form of the kernel.

By further substituting (4.5b) into (4.5a), we obtain:

$$t_0 = x_0^{1-\gamma}, \quad (4.6a)$$

or alternatively,

$$x_0 = t_0^{1/(1-\gamma)}. \quad (4.6b)$$

170 By further substituting (4.6b) into (4.4d), we also obtain:

$$n_0 = 1/t_0^{2/(1-\gamma)}. \quad (4.6c)$$

The transformations, (4.6a) and (4.6c), or (4.6a) and (4.4d), constitutes two possible pairs for defining the invariant transformations. In the following, we focus on the first pair, (4.6a) and (4.6c), for ease of interpretations, except the case with  $\gamma = 1$  when the transformation (4.6c) is ill-defined. In this case, we adopt the latter pair, (4.6a) and (4.4d).

175 The constraint (4.6a) suggests an invariant relation:

$$tx^{\gamma-1} = t^* x^{*\gamma-1}.$$

This invariant relation further suggests that these two independent variables,  $t$  and  $x$ , can be combined into a single independent variable:

$$\xi = tx^{\gamma-1}. \quad (4.7a)$$

180 In the following,  $\xi$  is principally interpreted as a transformed droplet mass.

In the same manner, the constraint (4.6c) suggests the invariant relation,

$$nt^{2/(1-\gamma)} = n^* t^{*2/(1-\gamma)}, \quad (4.8a)$$



and suggest to introduce a new dependent variable by

$$\nu = nt^{2/(1-\gamma)}. \quad (4.8b)$$

185 By combining those transformed variables, we expect that the general solution would take a form  $\nu = \nu(\xi)$ , or

$$n = t^{-2/(1-\gamma)}\nu(tx^{\gamma-1}). \quad (4.9)$$

Especially, when  $\gamma = 0$  and  $\gamma = 2$ , respectively, the above similarity solution (4.9) reduces to the form

$$n = \frac{\nu(x/t)}{t^2}, \quad (4.10a)$$

$$n = t^2\nu(xt). \quad (4.10b)$$

190 Note that  $\gamma = 0$  corresponds to the case that the kernel is constant, and  $\gamma = 2$  is obtained, for example, from the form,  $K = x^2 + y^2$ , as qualitatively expected for the cloud droplets (*cf.*, Long 1974). The first similarity solution (4.10a) is intuitive to interpret: a peak of the distribution moves towards a larger size linearly with time by keeping its distribution form, associated with a decrease of its peak value proportional to  $t^{-2}$ .

On the other hand, the second (4.10b) is even unphysical: a peak of distribution moves to a smaller size with  $t^{-1}$  associated with the increase of the peak value proportional to  $t^2$ . This unphysical nature of the solution can be amended first by realizing the SCE is also invariant by translation in time so that a constant time,  $t_0$ , can be subtracted from time in the solution above. Furthermore, re-defining the resulting  $\nu(t-t_0)$  as  $\nu(t_0-t)$ :

$$n = (t_0-t)^2\nu(x(t_0-t)). \quad (4.10c)$$

Here, although the final result may appear to be a consequence of inverting the time direction, the time inversion transformation is actually not applied in the derivation. After this transformation, the peak size of a distribution increases with time, and the maximum decreases with time. However, this solution collapses at a finite time,  $t = t_0$ , with the peak reaching the infinity. We expect that this solution is particularly only asymptotically valid as often the case with any similarity solutions (*cf.*, Barenblatt 1996).

Finally, when  $\gamma = 1$ , from Eq. (4.7a), we find

$$205 \quad \xi = t$$

suggesting that the evolution is primarily controlled by time,  $t$ . Combining this conclusion with Eq. (4.4d) suggests a general solution of the form:

$$n = \nu(t)/x^2. \quad (4.12)$$

Substitution of the form (4.12) into Eq. (2.1) further suggests that the problem reduces to the form

$$210 \quad \frac{d\nu}{dt} = \nu^2 S_0, \quad (4.13a)$$



where  $S_0$ , determined by the integral,

$$S_0 = \frac{x^2}{2} \int_0^x \frac{K(x-y, y)}{(x-y)^2 y^2} dy - \int_0^{+\infty} \frac{K(x, y)}{y^2} dy. \quad (4.13b)$$

Since  $\nu$  is the function of  $t$  only, it also follows that  $S_0$  must be a constant. Recall the asymptotic nature of the similarity solutions, thus  $S_0$  is also constant only under a certain asymptotic sense.

215 The differential equation (4.13a) is readily solved, and we find:

$$\nu = \frac{1}{1/\nu_0 + S_0 t} \quad (4.14)$$

with  $\nu = \nu_0$  at  $t = 0$ . However, the above time dependence is identical to Eq. (3.4) obtained by a separation of variables, but that is also contradicting with the assumption of separation of variables. The fact suggests that the solution (4.14) is valid only in a limited sense approximately. Note furthermore, for the total mass (Eq. 2.3b) to be conserved, the solution (4.12) must be  
220 valid only over a finite range, because otherwise the mass integral does not converge, as seen immediately below.

The integral of Eq. (4.13b) can also be readily performed, when the kernel,  $K$ , is also defined in a simple analytical form, yet with a difficulty of arriving a desired final result. Take for example, the form,  $K = x + y$ , as suggested by Long (1974) to be appropriate for the rain scale. As a result, the integral (4.13b) reduces to:

$$S_0 = \frac{x^3}{2} \int_0^x \frac{1}{(x-y)^2 y^2} dy - \int_0^{+\infty} \left( \frac{1}{y} + \frac{x}{y^2} \right) dy. \quad (4.15)$$

225 The two integrals can also be readily performed analytically in indefinite forms and:

$$\int \frac{1}{(x-y)^2 y^2} dy = -\frac{2}{x^2(y-x)} + \frac{1}{xy(y-x)} - \frac{2}{x^3} \log \left| \frac{y-x}{y} \right|,$$

$$\int \left( \frac{1}{y} + \frac{x}{y^2} \right) dy = -\frac{x}{y} + \log y.$$

However, the integrals become singular with given integral ranges. For this reason, we modify the integral ranges to  $[\epsilon, x - \epsilon]$  and  $[\epsilon, X]$ , respectively, assuming  $\epsilon$  and  $X$  to be a small and large parameters. As a result, these two integrals are performed  
230 into:

$$\int_{\epsilon}^{x-\epsilon} \frac{1}{(x-y)^2 y^2} dy = \frac{2}{\epsilon x^2} - \frac{2}{x^3} - \frac{4}{x^3} \log \frac{\epsilon}{x}, \quad (4.16a)$$

$$\int_{\epsilon}^X \left( \frac{1}{y} + \frac{x}{y^2} \right) dy = \left( \frac{1}{\epsilon} - \frac{1}{X} \right) x + \log \frac{X}{\epsilon}, \quad (4.16b)$$

where small contributions due to  $\epsilon$  are neglected. The main problem with these results is that direct substitution of them into Eq. (4.15) does not lead to a result with  $S_0$  a constant, but it depends on  $x$ .



235 Yet, this merely reflects the asymptotic nature of similarity solutions. An expected similarity solution is recovered only in the asymptotic limit of  $x \rightarrow 0$ , but also keeping the inequality,  $\epsilon \ll x$ . Thus, assuming,  $\epsilon \ll x \ll 1$  and  $X \gg 1$ , and retaining only the leading terms in the results of Eqs. (4.16a, b), we obtain

$$S_0 \simeq 2 \log \frac{1}{\epsilon} - \log \frac{X}{\epsilon} \quad (4.17)$$

from Eq. (4.15). Unfortunately, this final result is unclosed, because we still need to specify  $\epsilon$  and  $X$ .

240 In this manner, generally speaking, the integral,  $S_0$ , can be considered a constant only under a certain asymptotic limit. However, it may be worthwhile to note that a choice of the kernel,  $K$ , that makes  $S_0$  constant exists, which is:

$$K(x, y) = \frac{(A - 6S_0)x + (A + 6S_0)y}{(x + y)^4} x^2 y^2.$$

## 5 Similarity Solutions as Extension of Separation of Variables

In the last section, forms of similarity solutions have been inferred by directly identifying the invariant transformations arising from the symmetries of the given governing equation (SCE). An explicit asymptotic solution has also been sought under this approach. In the present section, in turn, we seek similarity solutions in a more explicit manner by taking an approach as a direct extension of the separation of variables considered in Sec. 3.

More precisely, we seek solutions of the form:

$$n = \tilde{N}(t) \tilde{n}(\xi) \quad (5.1a)$$

250 as a generalization of the form (3.1). Here,  $\xi$  is a variable depending on both  $x$  and  $t$ , intending to express the tendency that a peak of a distribution moves with time. In the following we consider the form:

$$\xi = \alpha(t)x, \quad (5.1b)$$

in which the time dependence of  $\alpha$  is to be determined. Eq. (5.1b) is essentially interpreted as a transformation of the size,  $x$ , into a general coordinate,  $\xi$ . This form is originally proposed by Friedlander (1961), further pursued by *e.g.*, Scott (1968) and Drake (1972), and reviewed in Secs. 11.7.2 and 15.3.2 of Pruppacher and Klett (1997).

The following two relations are immediately identified:

$$\frac{\partial n}{\partial t} = \tilde{n} \frac{\partial \tilde{N}}{\partial t} + \left( \xi \frac{\partial \tilde{n}}{\partial \xi} \right) \frac{\dot{\alpha}}{\alpha} \tilde{N}, \quad (5.2a)$$

$$K(x, y) = K(\xi/\alpha, \eta/\alpha) = \alpha^{-\gamma} K(\xi, \eta), \quad (5.2b)$$

setting  $\eta = \alpha y$  and recalling the relation (4.5b).



260 As in Sec. 2, we introduce the two normalization conditions

$$\int_0^{+\infty} \tilde{n}(\xi) d\xi = 1, \quad (5.3a)$$

$$\int_0^{+\infty} \xi \tilde{n}(\xi) d\xi = 1. \quad (5.3b)$$

These two constraints lead to the two relations for  $\tilde{N}$  and  $\alpha$ :

$$\tilde{N} = \alpha N, \quad \alpha^2 = \tilde{N}/m, \quad (5.4a, b)$$

265 where  $N$  and  $m$  are the total number density and the total mass, respectively. Recall that without loss of generality, we can set  $m = 1$ , and we find that both  $\tilde{N}$  and  $\alpha$  are determined from the total number density,  $N$ , by

$$\tilde{N} = N^2, \quad \alpha = N. \quad (5.5a, b)$$

Thus, the problem reduces to that of solving the two dependent variables,  $\tilde{N}$  and  $\tilde{n}$ , against the two independent variables,  $t$  and  $\xi$ , where  $\xi = Nx$ .

270 By using all the above relations, SCE (Eq. 2.1) reduces to:

$$(2\tilde{n} + \xi \frac{\partial \tilde{n}}{\partial \xi}) \frac{d}{dt} \left( \frac{N^2}{2} \right) = N^{-\gamma+2} S(\xi), \quad (5.6a)$$

where

$$S(\xi) = \frac{1}{2} \int_0^{\xi} \tilde{n}(\xi-\eta) \tilde{n}(\eta) K(\xi-\eta, \eta) d\eta - \tilde{n}(\xi) \int_0^{+\infty} \tilde{n}(\eta) K(\xi, \eta) d\eta \quad (5.6b)$$

plays a role of the source term in Eq. (5.6a). Note that Eq. (5.6a) is equivalent to Eq. (5) of Xie (2024).

275 Eq. (5.6a) is separated into the two equations by introducing a separation constant,  $\lambda$ :

$$\dot{N} = -\lambda N^{-\gamma+2}, \quad (5.7a)$$

$$2\tilde{n} + \xi \frac{\partial \tilde{n}}{\partial \xi} = -\frac{1}{\lambda} S(\xi). \quad (5.7b)$$

The time dependence of the system is obtained immediately by solving Eq. (5.7a):

$$N = [1 + (-\gamma + 1)\lambda t]^{-1/(-\gamma+1)}, \quad (5.8a)$$

280  $\tilde{N} = [1 + (-\gamma + 1)\lambda t]^{-2/(-\gamma+1)}, \quad (5.8b)$

when  $\gamma \neq 1$ , and exceptionally when  $\gamma = 1$ ,

$$N = e^{-\lambda t}, \quad (5.9a)$$

$$\tilde{N} = e^{-2\lambda t}. \quad (5.9b)$$



The eigenvalue,  $\lambda$ , is in principle, determined from the normalization conditions, (5.1a, b), and more specifically from the evolution equation of the total number density:

$$\lambda = \frac{1}{2} \int_0^{+\infty} \int_0^{+\infty} K(\xi, \eta) \tilde{n}(\xi) \tilde{n}(\eta) d\xi d\eta \quad (5.10)$$

as obtained by directly integrating Eq. (2.1) over  $x$ .

In the following, we consider solutions with the two special forms of kernel. Note that in the literature, further deductions of the system is pursued by transforming the time into a new variable,  $\tau$ , by

$$\tau = 1 - N(t) \quad (5.11)$$

(Sec. 11.3.2 of Pruppacher and Klett, 1997) especially when  $\gamma \neq 1$ . Here, we proceed without this transformation. The results in Sec. 5.2 has been originally obtained by this procedure.

### 5.1 When the kernel is constant

Let  $K = 1$ , then Eq. (5.10) leads to  $\lambda = 1/2$ , and Eqs. (5.8a, b) reduce to:

$$N = (1 + t/2)^{-1}, \quad \tilde{N} = (1 + t/2)^{-2}. \quad (5.12a, b)$$

The source term defined by Eq. (5.6b) reduces to:

$$S = \frac{1}{2} \int \tilde{n}(\xi - \eta) \tilde{n}(\eta) d\eta - \tilde{n}(\xi). \quad (5.13)$$

We solve Eq. (5.7b) by Laplace transformation, designating it as  $\mathcal{L}$ . First, applying the Laplace transform,  $\bar{S}$ , to Eq. (5.13):

$$\bar{S} \equiv \mathcal{L}[S] = \int_0^{+\infty} S e^{-p\xi} d\xi = \frac{\bar{n}^2}{2} - \bar{n}$$

invoking a well known formula for the Laplace transform of a convolution,

$$\mathcal{L}\left[\int_0^\xi f(\xi - \eta)g(\eta)d\eta\right] = \bar{f}\bar{g},$$

where the overbar designated the Laplace transform.

In performing the Laplace transform on the left-hand side of Eq. (5.8b), we note another formula:

$$\frac{\partial \bar{f}}{\partial p} = - \int_0^{+\infty} \xi f e^{-p\xi} d\xi.$$

By performing an integral by part, and applying the above formula,

$$\int_0^{+\infty} \xi \tilde{n} e^{-p\xi} d\xi = -(\bar{n} + p \frac{\partial \bar{n}}{\partial p}).$$



With the help of those results, by Laplace transform, Eq. (5.7b) reduces to

$$\frac{\partial}{\partial p}(p\bar{n}) = \bar{n}^2,$$

which leads to a solution,  $\bar{n} = \beta/(p + \beta)$ , with  $\beta$  a constant. After inverse transform, we find :

$$310 \quad \tilde{n} = e^{-\xi}, \tag{5.12c}$$

where  $\beta = 1$  by the normalization condition (5.3a).

By putting Eqs. (5.12a, b, c) together,

$$n = \frac{e^{-x/(1+t/2)}}{(1+t/2)^2}. \tag{5.14}$$

This solution is originally obtained by Schumann (1940) and reproduced in Sec. 11.7.2 of Prepecher and Klett (1997). Note also that with  $t \rightarrow \infty$ , the above solution asymptotically approaches to the invariant solution (4.10a) with  $\nu(\xi) = e^{-2\xi}$ . Thus, Eq.. (5.14) constitutes a special case of the solution (4.10a).

## 5.2 When $\gamma = 1$ :

In this case, the solutions for  $N$  and  $\tilde{N}$  are already given by Eqs. (5.9a, b). Letting  $K = x + y$ , Eq. (5.10) leads to  $\lambda = 1$ , thus  $\xi = xe^{-t}$ , and the source term defined by Eq. (5.6b) reduces to:

$$320 \quad S = \frac{\xi}{2} \int_0^{\xi} \tilde{n}(\xi - \eta) \tilde{n}(\eta) d\eta - (1 + \xi) \tilde{n}(\xi).$$

The Laplace transform of the above is:

$$\bar{S} = -\frac{1}{2} \frac{d}{dp} \bar{n} - \left(-\frac{d}{dp} + 1\right) \bar{n}.$$

Thus, Eq. (5.8b) reduces by Laplace transform to:

$$-\left(\bar{n} + p \frac{d\bar{n}}{dp}\right) + \bar{n} = \frac{1}{2} \frac{d}{dp} \bar{n}^2 + \left(-\frac{d}{dp} + 1\right) \bar{n},$$

325 or

$$(\bar{n} + p - 1) \frac{d\bar{n}}{dp} = 0.$$

It gives the two possible solutions,  $d\bar{n}/dp = 0$  and  $\bar{n} = 1 - p$ .

i) When  $d\bar{n}/dp = 0$ :  $\bar{n}$  is a constant in this case, and its inverse transform leads to  $\tilde{n}(\xi) = \delta(\xi)$ , taking into account the normalization condition. Substituting  $\xi = xe^{-t}$  to this solution, we find  $\tilde{n} = e^t \delta(x)$ . Combining it with Eq. (5.9b), the full solution is:

330

$$n = \delta(x) \tag{5.15a}$$



*i.e.*, all the particles just stay at the state of the zero size: it is not physically meaningful.

ii) When  $\bar{n} = 1 - p$ : There is no readily available inverse transform formula. Yet, we note that when  $p \ll 1$ , this solution may be approximated as  $\bar{n} \simeq e^{-p}$ . This form can be readily transformed backwards, and we obtain  $\tilde{n} \simeq \delta(\xi - 1)$ . By substituting  $\xi = xe^{-t}$ ,  $\tilde{n} \simeq e^t \delta(x - e^t)$ , and the full solution is:

$$n = \delta(x - e^t) \tag{5.15b}$$

*i.e.*, the initial droplet of the size  $x = 1$  exponentially grows with time without any broadening of the distribution. This solution is expected to be valid for the asymptotic limit of  $t \rightarrow +\infty$  being obtained with an approximation of  $p \ll 1$  under the Laplace transform. Yet, this solution is rather speculative, and direct numerical experiments in the next section simply fail to suggest any validity.

On the other hand, an exact analytical solution is obtained (*e.g.*, Golovin 1963, Scott 1968) by an additional transformation of time given by Eq. (5.11):

$$n(x,t) = \frac{(1 - \tau)e^{-(1+\tau)m}}{m\sqrt{\tau}} I_1(2m\sqrt{\tau}), \tag{5.16}$$

where  $n(x,0) = e^{-m}$ ,  $\tau = 1 - e^{-t}$ , and  $I_1$  is the first-order modified Bessel function of the first kind. Grigoriev and Meleshoko (1995) further show that how general invariant solutions for SCE is obtained by exploiting the transformation (5.11) systematically. See Grigoriev *et al.* (2010) for more general discussions.

## 6 Numerical Experiments

Over the last two sections, we have pursued the two approaches for deriving the similarity solutions for the SCE: the symmetry analysis and the generalized separation of variables. In the following, we focus on the numerical verification of the general invariant solutions (4.10a, c) derived in Sec. 4. In the last section, in the case with  $\gamma = 0$ , a special solution (5.14) with the form of Eq. (4.10a) is derived, in support of the validity of the given invariant solution. In the case with  $\gamma = 1$ , two qualitatively different solutions are identified. However, we have simply failed to reproduce those solutions in any approximate sense numerically along the line of following numerical experiments.

In the following, the SCE system is considered in nondimensional units with all the variables also normalized properly. More specifically, all the constants for the kernels,  $K(x,y)$ , are set unity, and the mass distributions,  $n(x)$ , are normalized to unity by integration. Using typical values,  $K_0 = 10^{-3} \text{ cm}^3\text{s}^{-1}$  and  $N_0 = 200 \text{ cm}^{-3}$ , we find a typical time scale of the system to be:

$$\tau = 1/K_0 N_0 = 5 \text{ sec.}$$

This is the unit of the nondimensional time in the following numerical experiments.

For the purpose of those numerical experiments, we consider three types of idealized kernel forms:

i)  $\gamma = 0$ :  $K(x,y) = 1$ .



ii)  $\gamma = 1: K(x, y) = x + y.$

iii)  $\gamma = 2: K(x, y) = x^2 + y^2.$

According to Long (1974), the last two forms are conceptually applicable to the cloud and rain droplets, respectively.

365 The initial mas distribution,  $n$ , is either the Gaussian or Gamma distribution, as given respectively by:

$$n = \left(\frac{\lambda}{\pi}\right)^{1/2} \exp[-\lambda(x - x_0)^2], \quad (6.1a)$$

$$n = \frac{\lambda^{\mu+1}}{\Gamma(\mu+1)} x^\mu e^{-\lambda x}, \quad (6.1b)$$

where  $\lambda$ ,  $x_0$ , and  $\mu$  are the free parameters in the distributions.

370 The adopted numerical algorithm is as described in Bott (1998), and we use the code provided by the original author for our computations with minor modifications: to truncate the kernel to zero with the choice of  $\gamma = 2$  to the maximum value of  $10^6$  to avoid an unwanted overflow in computations. The mass range considered for the present study is from  $x = 1.2 \times 10^{-9}$  to  $x = 1.2 \times 10^{+36}$ , although we will only show a limited range with significant mass densities in the following plots. The default time step is  $\Delta t = 0.1$  except for the case with  $\gamma = 2$  requires a much shorter time step with  $\Delta t = 10^{-3}$  due to the large values of kernel for the large  $x$ .

375 In the following computations, we will find a general tendency of the distribution to approach similarity solutions, especially, as predicted from the symmetry analysis in Sec. 4. According to the analysis therein, the distribution should approach to a universal form,  $\nu(\xi)$ , asymptotically as  $t \rightarrow \infty$ . Here, the predicted universal form,  $\nu(\xi)$ , is obtained by re-scalings:

i) For  $\gamma = 0$ :

$$\nu(\xi) = t^2 n(x, t), \quad \xi = x/t. \quad (6.2a, b)$$

380 i) ii) For  $\gamma = 1$ :

$$\nu(\xi) = x^2 n(x, t), \quad \xi = t. \quad (6.3a, b)$$

i) iii) for  $\gamma = 2$ :

$$\nu(\xi) = n(x, t)/(t_0 - t)^2, \quad \xi = x(t_0 - t). \quad (6.4a, b)$$

Here, a time constant,  $t_0$ , suggests a time that the given distribution “collapses”.

385 The following numerical examples are highly selective, but intend to suggest a general behavior for each choice of  $\gamma$ . With each figure for those examples, the top frame (a) is always the distribution,  $n(x, t)$ , and (b) is the re-scaled universal distributing,  $\nu(\xi)$ .

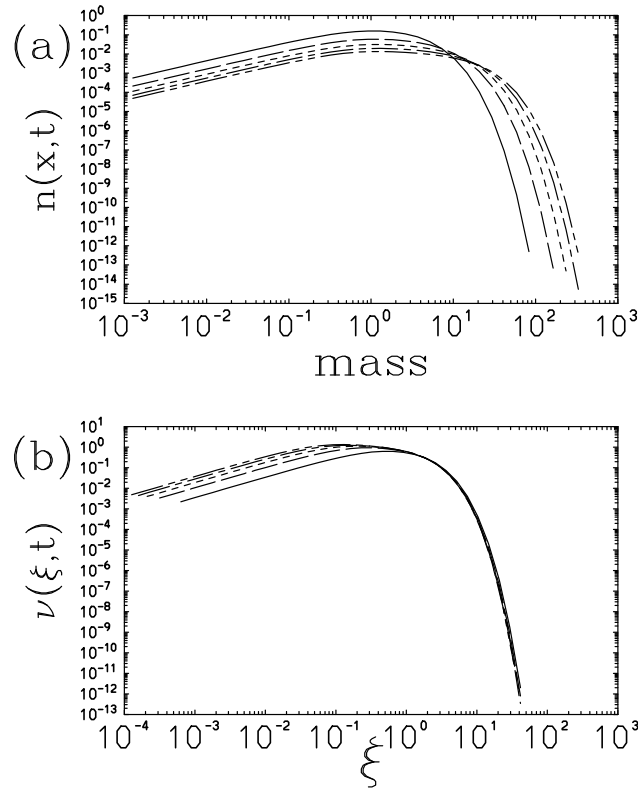


**Figure 1.** The case with  $\gamma = 0$ , initialized by the gamma distribution with  $\lambda = \mu = 1$ : (a) The distribution,  $n(x, t)$ , (b) Rescaled distribution,  $\nu(\xi, t)$ : from  $t = 1$  with every  $\Delta t = 2$ . The curve at  $t = 1$  is shown in solid. The re-scaled abscissa in (b) is defined by  $\xi = x/t$ .

### 6.1 The Case with $\gamma = 0$ :

First to consider is the case with  $\gamma = 0$  so that the kernel,  $K$ , is a constant, *i.e.*,  $K = 1$ . The results of numerical time integrations are shown in Figs. 1–3: the first two cases are initialized with gamma distributions, and the third with the Gaussian distribution.

Fig. 1 (a) shows the case initialized with the gamma distribution (6.1a) with  $\lambda = \mu = 1$ : due to the coalescence growth of droplets, the overall distribution evolves to the larger sizes with time with the overall density decreasing, because the coalescence also lead to less number of droplets with time. Fig. 1 (b) shows the same, but after rescaling the distribution by Eq. (6.2a, b) into  $\nu$  as a function of  $\xi$ . As time increases, the distribution collapses into a single curve: with the larger droplet sizes, almost immediately, but with the smaller droplet sizes, rather gradually. However, keep in mind that by taking a logarithmic scale in the horizontal axis, we visualize the relative convergence of the curve, but realize that the absolute difference is almost negligible in the direction of  $\xi$ .

Fig. 2 shows the case when the initial gamma distribution parameters are re-set to  $\lambda = 4$  and  $\mu = 4$ : the distribution presents a sharper peak at  $x = 1$  as a result. Yet, the overall evolution follows that of Fig. 1: the distribution grows towards the larger

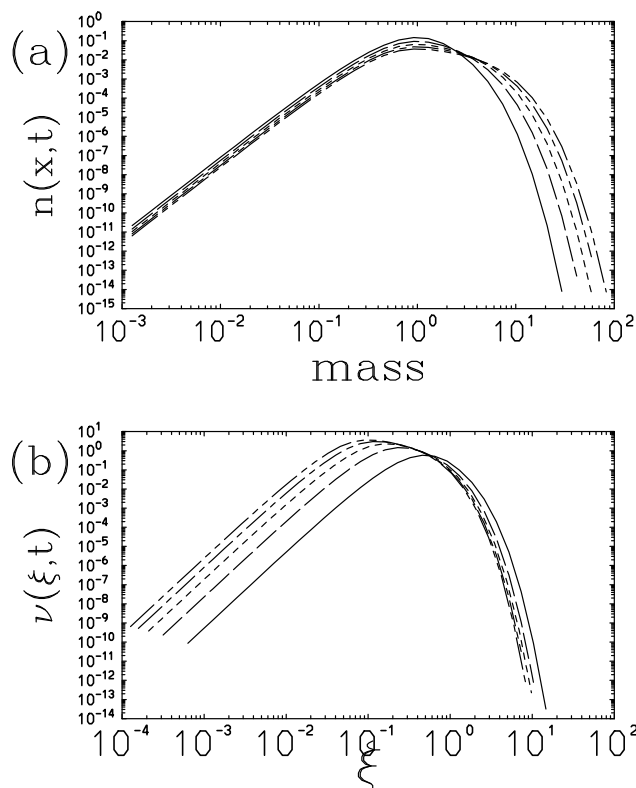


**Figure 2.** The same as Fig. 1, but with  $\lambda = 4$  and  $\mu = 4$ .

400 masses with time (Fig. 2(a)). However, the tendency for an overall decrease of the number density is less visible. After rescaling (Fig. 2(b)), the distribution collapses almost to a single curve, but in this case, some spread is visible.

The overall evolution of the Gaussian case does not sensibly depend on the choice of the parameter,  $\lambda$ . Fig. 3 shows an example: the distribution continuously spreads with time (a). Yet, the positive tail part relatively rapidly converges to a universal transformed distribution (b). However, with the smaller values of  $\lambda$ , the computations somehow tend to be unstable, and the  
 405 solution typically break down around  $t \simeq 1$ .

## 6.2 The Case with $\gamma = 1$ :

As a first example of the case with the kernel parameter,  $\gamma = 1$ , Fig. 4 shows the case initialized with the gamma distribution with  $\lambda = \mu = 1$ . As seen in Fig. 4(a), in general, the distribution spreads to the larger masses with time, more extensively than the cases with  $\gamma = 0$ , with the positive tail stretches longer with time.

410 Note that in this case, the universal function,  $\nu(t)$ , obtained by multiplying  $x^2$  on the original mass distribution,  $n(x, t)$ , is expected to become a function of time only (*cf.*, Eqs. 6.3a, b). It follows that, when  $\nu(t)$  is plotted as a function of  $x$  as shown in (b),  $\nu$  is expected to become a constant. The simulation indeed suggests that the positive tail part asymptotically approaches

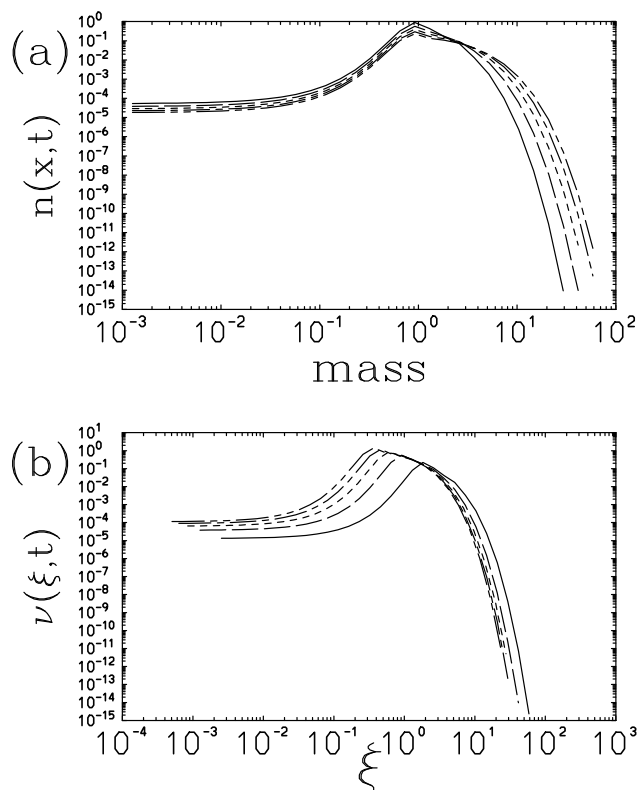


**Figure 3.** The same as Figs. 1 and 2, but initialized by the Gaussian distribution with  $\lambda = 10$  and  $x_0 = 1$ , and the interval of  $\Delta t = 0.5$  with the initial curve at  $t = 0.5$  (solid). The initial condition (not shown) immediately spreads out over an initial time step, regardless of its choice. The case shown here is with the time step,  $\delta t = 10^{-2}$ .

a constant with time, however with a weakly increasing tendency. Note that this defect may partially be attributed to an implicit numerical diffusion in the scheme, that makes the slope less steep. Also note that the whole distribution represented by the transformed density,  $\nu(t)$ , gradually decreases with time, by qualitatively following Eq. (4.14). 415

Fig. 5 is the same as Fig. 4, but the increase over the smaller droplet sizes initially is steeper with  $\mu = 2$ , and with a better defined maximum. Nevertheless, the evolution dominated at the larger droplet sizes is very similar to that of Fig. 4.

The similar behaviors also follow for the case initialized with the Gaussian distribution. Fig. 6 shows an example: the evolution tendency remains almost identical with changing the steepness of the initial Gaussian, because the initial steep peak 420 rapidly collapses, and it approaches a universal distribution, associated with a gradual extension of the distribution to the larger masses.

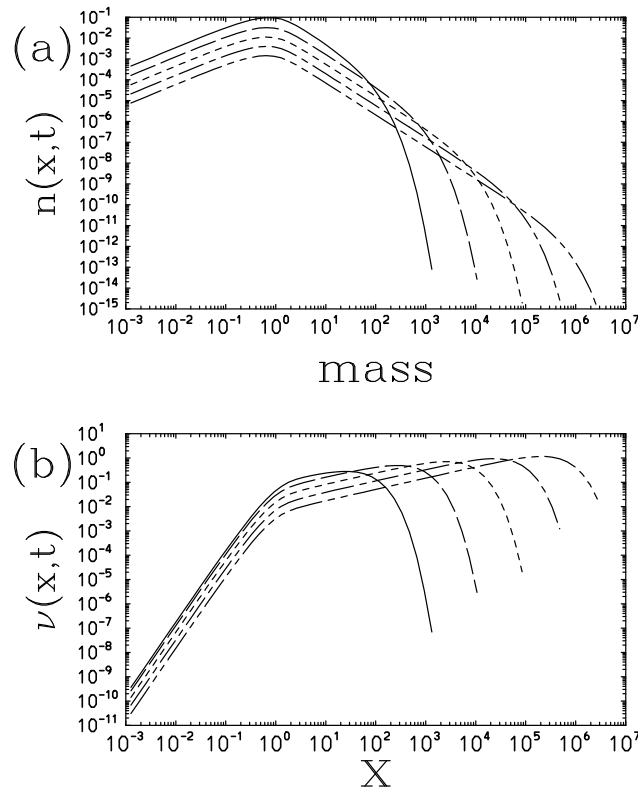


**Figure 4.** The case with  $\gamma = 1$ , initialized by the gamma distribution with  $\lambda = \mu = 1$ : (a) The distribution,  $n(x, t)$ , (b) Rescaled distribution,  $\nu(\xi, t) = x^2 n(x, t)$ : from  $t = 0.5$  with every  $\Delta t = 0.5$ . The curve at  $t = 0.5$  is shown in solid.

### 6.3 The Case with $\gamma = 2$

With  $\gamma = 2$ , the asymptotic analysis in Sec. 4 predicts that the distribution collapses at an unspecified time,  $t_0$ . However, the numerical results shown in Figs. 7 and 8 do not show that the distribution literally “collapses” into a universal solution towards a finite time,  $t \rightarrow t_0$ . Rather the rules (6.4a, b) transform the distributions at different separate times,  $t - t_0$ , tend to collapse into a single distribution, as suggested in the frame (b) for the distributions at  $t \geq 0.2$  for small  $\xi = x(t_0 - t)$  both in Figs. 7 and 8. The tendency for this “collapse” is, however, not homogeneous, and the expected overlapping happens more preferably with the smaller mass values.

## 7 Conclusions

430 Diffusion growth beyond the activation point is relatively slow. A more efficient growth is achieved by mutual collisions of the droplets leading to mergers. This process is described by the so-called the stochastic collection equation. We have examined the basic behavior of the stochastic collection equation from the perspectives of symmetries.

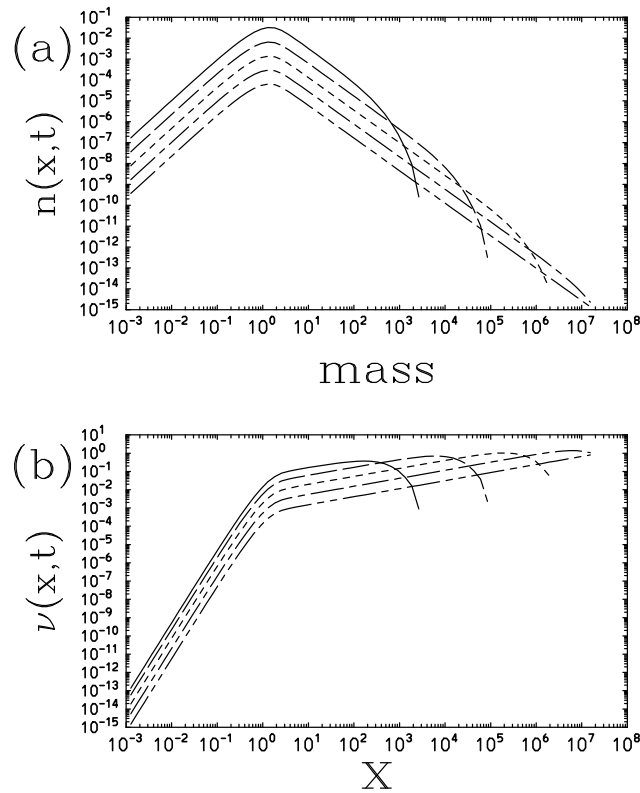


**Figure 5.** The same as Fig. 4, but with  $\mu = 2$ : (a) The distribution,  $n(x, t)$ , (b) Rescaled distribution,  $\nu(\xi, t)$ : from  $t = 0.5$  with every  $\Delta t = 0.5$ . The curve at  $t = 0.5$  is shown in solid.

The present paper has investigated the stochastic collection equation (SCE) in standalone manner, when no other physical process contributes, further assuming that collision kernel form is independent of the droplet size. As a result, SCE becomes scale invariant, *i.e.*, the evolution of the droplet population represents the same characteristic regardless of, say, the peak droplet size after a proper rescaling, and the given droplet population evolution remains a valid solution of the SCE even after any rescaling. An important corollary of this statement is that we do not observe any transformation in the characteristics of the droplet–size distribution as the droplets grow. Especially, there is no distinction between the cloud and rain droplets arises.

Invariant solutions derived by symmetry analysis in Sec. 4 have been numerically verified in Sec. 6 as asymptotic tendencies towards  $\xi \rightarrow \infty$  with the kernel symmetry with  $\gamma = 0$  and 1. Especially, in the case with  $\gamma = 1$ , the normalized distribution,  $\nu = x^2 n$ , asymptotically approaches constant with time as predicted by the invariant solution predicts, albeit a remaining weak increasing tendency with  $x$  likely due to a numerical issue. On the other hand, the invariant solution derived with  $\gamma = 2$  is re–interpreted as a tendency of distributions to collapse into a single distribution by the transformations by Eqs. (6.4a, b).

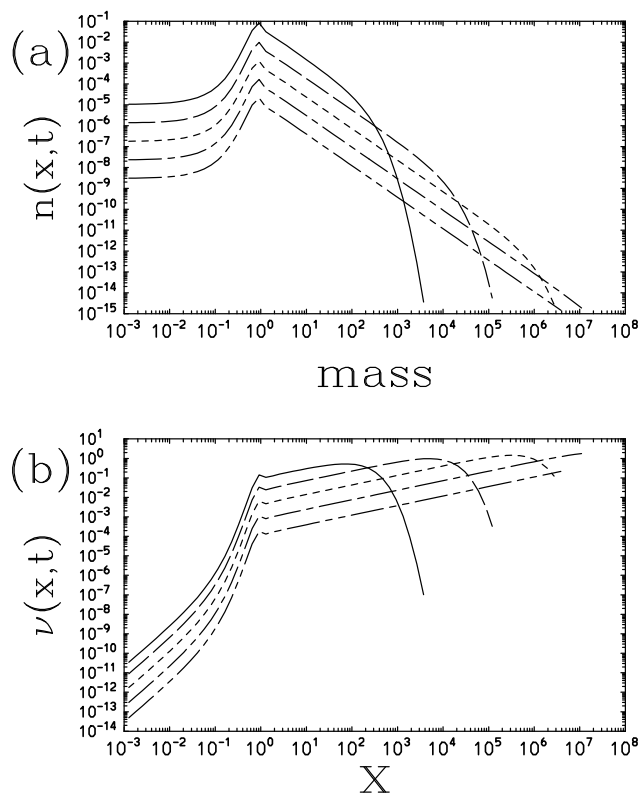


**Figure 6.** The same as Figs. 4 and 5, but initialized by the Gaussian distribution with  $\lambda = 10$  and  $x_0 = 1$ , with the interval of  $\Delta t = 2$  with the initial curve for  $t = 2$  (solid). The initial condition spreads out relatively fast. The distribution continuously spreads with time (a). Yet, positive tail part relatively rapidly converges to a universal transformed distribution (b).

The results with the symmetry analyses have further motivated us to pursue solutions with separations of variables in terms of time,  $t$ , and the transformed mass,  $\xi$ , in Sec. 5. The analysis of the case with  $\gamma = 1$  lead to new asymptotic solutions. However, numerical simulations in Sec. 6 fail to prove the relevance of those solutions.

The most basic conclusion from the present study is that the form of the collection kernel defines the equilibrium droplet-size distribution. Earlier studies by Berry (1967), and Berry and Reinhardt (1974c, d) suggested that derivatives of the kernel in respect to the droplet sizes define the distribution. According to the present study, it is more precisely, the symmetry characteristics of the kernel in respect to the droplet sizes, that determine the asymptotic tendency of the size distribution with time. Although only the idealized cases are considered in the study, we emphasize the generality of the methodology, which can equally applied to more realistic settings.

*Code availability.* All the fortran codes used for the present study is available by request to the first author.

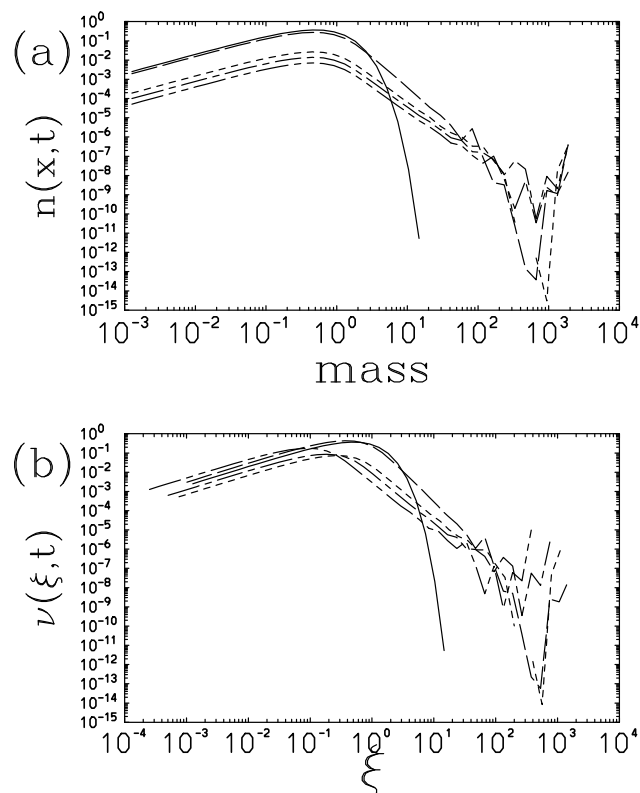


**Figure 7.** The case with  $\gamma = 2$ , initialized by the gamma distribution with  $\lambda = \mu = 1$ : (a) The distribution,  $n(x, t)$ , (b) Rescaled distribution,  $\nu(\xi, t)$  with  $t_0 = 1$ : for  $t = 0$  (solid) and 0.2 (long dash) with the subsequent curves in the interval of  $\Delta t = 0.2$ .

*Author contributions.* The present study has been envisioned by MPHA, and principally performed by JIY with extensive inputs by MW.

455 *Competing interests.* The authors declare that they have no conflict of interest.

*Acknowledgements.* The numerical code for SCE has been kindly provided by Andreas Bott.

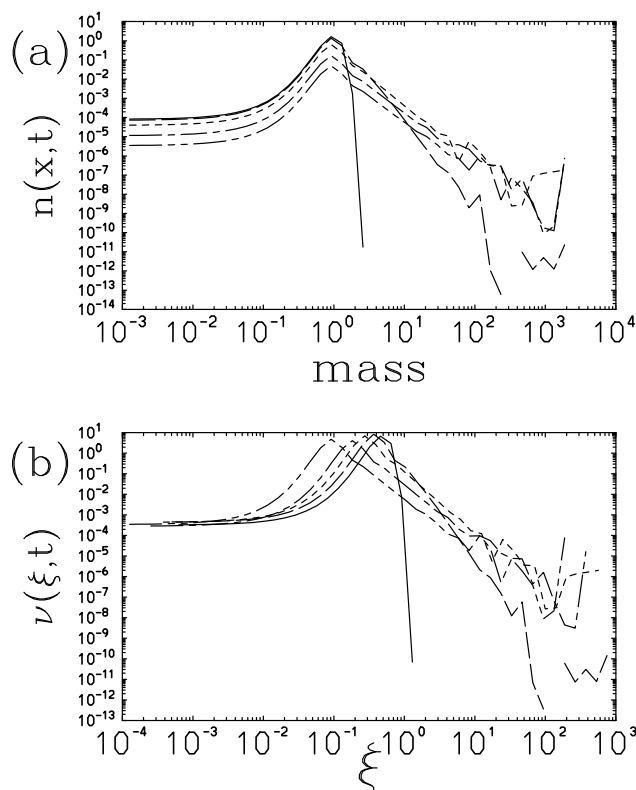


**Figure 8.** The same as Fig. 7, but initialized with the Gaussian distribution with  $\lambda = 10$  and  $x_0 = 1$ , with the interval of  $\Delta t = 0.1$ , and  $t_0 = 0.5$ . The first curve is at  $t = 0$  (solid).

## References

- Barenblatt, G. I., 1996: *Scaling, Self-Similarity, and Intermediate Asymptotics*, Cambridge University Press, Cambridge, UK, 386pp.
- Berry, E. X., 1967: Cloud droplet growth by collection. *J. Atmos. Sci.*, **24**, 688–701.
- 460 Berry, E. X., and R. L. Reinhardt 1974a: An analysis of cloud drop growth by collection: Part I. Double distribution. *J. Atmos. Sci.*, **31**, 1814–1824.
- Berry, E. X., and R. L. Reinhardt 1974b: An analysis of cloud drop growth by collection: Part II. Single initial distribution. *J. Atmos. Sci.*, **31**, 1825–1831.
- Berry, E. X., and R. L. Reinhardt 1974c: An analysis of cloud drop growth by collection: Part III. Accretion and self-collection. *J. Atmos.*  
 465 *Sci.*, **31**, 2118–2126.
- Berry, E. X., and R. L. Reinhardt 1974d: An analysis of cloud drop growth by collection: Part IV. A new parameterization. *J. Atmos. Sci.*, **31**, 2127–2135.
- Bluman, G. W., and S. Kumei, 1989: *Symmetries and Differential Equations*. Elsevier, New York, 412pp.
- Bott, A., 1998: A flux method for the numerical solution of the stochastic collection equation. *J. Atmos. Sci.*, **55**, 2284–2293.



- 470 Drake, R. L., 1972: The scalar transport equation of coalescence theory: Moments and kernels. *J. Atmos. Sci.*, **29**, 537–547.  
[https://doi.org/10.1175/1520-0469\(1972\)029<0537:TSTEOC>2.0.CO;2](https://doi.org/10.1175/1520-0469(1972)029<0537:TSTEOC>2.0.CO;2).
- Friedlander, S. K., 1961: Theoretical considerations for the particle size spectrum of stratospheric aerosol. *J. Meteor.*, **18**, 753–739.  
[https://doi.org/10.1175/1520-0469\(1961\)018<0753:TCFTPS>2.0.CO;2](https://doi.org/10.1175/1520-0469(1961)018<0753:TCFTPS>2.0.CO;2).
- Fournier, N., and P. Laurençot, 2006: Well-posedness of Smoluchowski’s coagulation equation for a class of homogeneous kernels. *J. Funct.*  
475 *Anal.*, **233**, 351–379.
- Golovin, A. M., 1963: The solution of the coagulation equation for cloud droplets in a rising air current. *Bull. Accd. Sci. SSSR Geophys. Ser.*  
(English translation), 482–487.
- Grigoriev, Y. N., and V. Meleshko, 1995: Group analysis of kinetic equations. *Russ. J. Anal. Math. Modeling*, **10**, 425–447.
- Grigoriev, Y. N., N. H. Ibragimov, V. F. Kovalev, and S. V. Meleshko, 2010: *Symmetries of Integro–Differential Equations: With Application*  
480 *in Mechanics and Plasma Physics*, Springer, Heidelberg, 305pp.
- Lin, F., Y. Yang, X. Yang, and Q. Zhang, 2024: Preliminary group classification and exact solutions of Smoluchowski equation with a source.  
*J. Comp. App. Math.*, **444**, 115770.
- Long, A., 1974: Solutions to the droplet collection equation for polynomial kernels. *J. Atmos. Sci.*, **31**, 1040–1052.
- Pruppacher, H. R., and J. D. Klett, 1997: *Microphysics of Clouds and Precipitation, Second Revised and Enlarged Edition with an Introduc-*  
485 *tion to Cloud Chemistry and Cloud Electricity*, Kluwer Academic Publishers, Dordrecht, 954pp.
- Schumann, T. E., 1940: Theoretical aspects of the size distribution of fog particles. *Quator. J. Roy. Meteor. Soc.*, **66**, 195–207.
- Scott, W. T., 1968: Analytic studies of cloud droplet coalescence I. *J. Atmos. Sci.*, **25**, 54–65
- Smoluchowski, M., 1917: Versuch einer mathematischen Theorie der koagulations–kinetic kolloider Losunger. *Z. Phs. Chem.*, **92**, 129–168.
- Strivastava, R., 1988: On the scaling of equations governing the evolution of droplet size distribution. *jas*, **45**, 1091–102.
- 490 Twomey, S., 1964: Statistical effects in the evolution of a distribution of cloud droplets by coalescence. *J. Atmos. Sci.*, **21**, 553–557.
- Twomey, S., 1966: Computations of rain formation by coalescence. *J. Atmos. Sci.*, **23**, 405–411.
- Xie, M., 2024: Comment on “Theoretical aspects of the size distribution of fog particles”. *Quator. J. Roy. Meteor. Soc.*, **150**, 3196–3120.